

# ac Josephson effect in asymmetric superconducting quantum point contacts

Shin-Tza Wu\* and Sungkit Yip

*Institute of Physics, Academia Sinica, Nankang, Taipei 115, Taiwan*

(Dated: September 17, 2018)

We investigate ac Josephson effects between two superconductors connected by a single-mode quantum point contact, where the gap amplitudes in the two superconductors are unequal. In these systems, it was found in previous studies on the dc effects that, besides the Andreev bound-states, the continuum states can also contribute to the current. Using the quasiclassical formulation, we calculate the current-voltage characteristics for general transmission  $D$  of the point contact. To emphasize bound versus continuum states, we examine in detail the low bias, ballistic ( $D = 1$ ) limit. It is shown that in this limit the current-voltage characteristics can be determined from the current-phase relation, if we pay particular attention to the different behaviors of these states under the bias voltage. For unequal gap configurations, the continuum states give rise to non-zero sine components. We also demonstrate that in this limit the temperature dependence of the dc component follows  $\tanh(\Delta_s/2T)$ , where  $\Delta_s$  is the smaller gap, with the contribution coming entirely from the bound state.

PACS numbers: 74.80.Fp, 74.50.+r

## I. INTRODUCTION

When a thin normal layer separates two superconductors, the superconducting coherence can spread across the normal region. The (dc and ac) Josephson effects are typical manifestations of such phenomena.<sup>1</sup> The rise of mesoscopic physics leads to reconsideration of these effects in systems where the normal region consists of narrow channels with quantized transverse modes (quantum point contacts). Typically the superconductors are connected via quantum point contacts which can be constrictions in semiconductor heterostructures<sup>2</sup> or atomic contacts in break junctions.<sup>3</sup> One of the insights gained from these studies is the important role of the Andreev bound-states in the Josephson effects.<sup>4</sup>

When a particle (hole) incident from a normal metal into a superconductor (or vice versa), besides normal reflections, the particle (hole) can be retro-reflected along its incident path and converted into a hole (particle). This is called the Andreev reflection. In superconductor-normal-metal-superconductor junctions, particles (and likewise for holes) can be reflected by the two NS interfaces repeatedly and form bound states in the normal region, which are the Andreev bound-states. For each transmission channel, there can be a pair of Andreev bound-states which carry currents in opposite directions. In dc Josephson effects, these bound states are responsible for carrying the supercurrent.<sup>4</sup> However, it is also known that for unequal gap junctions the Andreev bound-states can be missing for some ranges of phase difference.<sup>5,6</sup> In this case, the supercurrent is then carried entirely by the continuum states and the thermal noise of the current exhibits dramatically different features.<sup>6</sup>

Previously, ac effects in asymmetric junctions have been considered using the scattering matrix approach.<sup>7</sup> In these works, the authors focused on the characterization of the additional subgap structures due to the presence of two superconducting gaps and on the possible scheme for the measurement of the phase difference.<sup>7</sup> In this article, we shall instead concentrate on the *dynamics* of the Andreev bound-states in the ac effects at low bias. As pointed out by Averin and Bardas,<sup>8</sup> in this limit the dynamics of Andreev bound-states play a key role in the ac effects. Since for unequal gap junctions the Andreev bound-states can be missing for some ranges of phase difference,<sup>6</sup> it is therefore of interest to investigate its consequence in the ac effect.

We shall study the ac Josephson effect in unequal-gap superconducting quantum point contacts using the quasiclassical Green's function method.<sup>9</sup> This approach has previously been applied to the study of ac effects in symmetric junctions.<sup>10</sup> Here, we shall examine for asymmetric junctions the current-voltage characteristics at arbitrary transmission coefficients in the point contact. We will then study in detail the low bias regime where inelastic scattering rate is vanishingly small (compared with the bias voltage and the gap amplitudes).<sup>11,12</sup> Under this situation, similar to the dc effects in unequal-gap junctions,<sup>5,6</sup> the current receives contributions from both the Andreev bound-states and the continuum states (see Fig. 1). We shall show that in this limit the current-voltage characteristics can be understood from the current-phase relation provided the different behaviors of the bound states and the continuum states are taken into account. For unequal gap configurations, where the Andreev bound-states are missing for some ranges of phase difference, the continuum states give rise to non-zero sine components. Finally we will demonstrate that in the low bias limit the temperature dependence of the dc component is determined from the quasi-particle occupations at the smaller gap. In the Appendix

---

\*current address: Department of Physics, National Chung-Cheng University, Chiayi 621, Taiwan

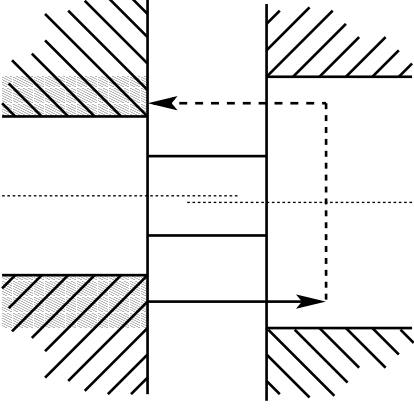


FIG. 1: Schematics of the asymmetric junction at low bias. The dotted lines at the center of the energy gaps depict the chemical potentials of the superconducting banks. The pair of discrete states in the normal region are the Andreev bound states. The gray areas indicate the continuum states that can contribute to the current, for instance, via Andreev reflections illustrated by the arrows [with a particle (solid arrow) converted into a hole (dashed arrow)].

we provide details needed for the calculation.

## II. FORMULATION

We consider two  $s$ -wave superconductors connected by a single-mode quantum point contact, which has transmission probability  $D$ . We shall assume that the point contact is short compared with the coherence lengths of the two superconductors. The order parameters of the left and right superconducting electrodes are, respectively,  $\Delta_l$  and  $\Delta_r \exp(i\phi)$ , where  $\Delta_{l,r}$  are taken to be real positive. Without loss of generality, we shall assume  $\Delta_l \leq \Delta_r$ . The junction is brought out of equilibrium by connecting the right electrode to a voltage source at fixed bias  $V$ , while the left electrode is grounded.

In the quasiclassical Green's function approach to superconductivity,<sup>9</sup> one reduces the Nambu Green's function by first separating the fast (relative) and slow (center of mass) degrees of freedom. Since for low energy phenomena the relevant time scale is much longer than the inverse of the Fermi energy. One can remove the irrelevant (fast) degrees of freedom by integrating out the magnitude of the relative momentum, retaining only the angular information specified by the unit vector  $\hat{\mathbf{p}}$  of the relative momentum. This leads to the quasiclassical Green's function  $\check{g}(\hat{\mathbf{p}})$ , which is in general an  $8 \times 8$  matrix in the Keldysh $\otimes$ spin $\otimes$ particle-hole space (see Appendix). Here, for brevity, we have omitted the time and frequency variables. For clean superconductors, the Green's function satisfies the equation of motion<sup>9</sup>

$$[\epsilon \tilde{\tau}_3 - \check{\Delta}, \check{g}] + i \mathbf{v}_F \cdot \nabla \check{g} = 0, \quad (1)$$

where  $\mathbf{v}_F$  is the Fermi velocity,  $\check{\Delta}$  the off-diagonal self-

energy (or the pairing function), and  $\tilde{\tau}_3$  the Pauli matrix (see Appendix for details). As usual,  $[\check{a}, \check{b}] \equiv \check{a}\check{b} - \check{b}\check{a}$  is the commutator and all products here involve matrix multiplications and convolutions in energy variables,<sup>9</sup> which have been omitted for brevity. Besides the equation of motion (1), the Green's function has to satisfy the normalization condition  $(\check{g})^2 = -\pi^2 \check{1}$  and appropriate boundary conditions.<sup>13</sup> Similar to the equilibrium case,<sup>6</sup> the current can be expressed in terms of the difference between quasiclassical Green's functions along the incident ( $\hat{\mathbf{p}}$ ) and the reflected ( $\hat{\mathbf{p}}$ ) directions near the interface  $\check{d} \equiv \check{g}(\hat{\mathbf{p}}) - \check{g}(\hat{\mathbf{p}})$ . The quantity  $\check{d}$  can be solved analytically and yields<sup>13,14</sup>

$$\check{d} = \frac{iD}{2\pi} [\check{g}_r, \check{g}_{l,\infty}] \left( 1 + \frac{D}{4\pi^2} (\check{g}_r - \check{g}_{l,\infty})^2 \right)^{-1}. \quad (2)$$

The Green's function for the left electrode  $\check{g}_{l,\infty}$  remains its equilibrium form while  $\check{g}_r$  for the right electrode now depends on the bias  $V$  (see Appendix).

In the quasiclassical formulation, the current can be expressed (we take  $\hbar = 1$ , the charge of electron  $e$ , and the electric current from right to left electrodes positive)

$$I(t) = \frac{e}{4\pi i} \int_{-\infty}^{\infty} \frac{d\epsilon}{2\pi} \int_{-\infty}^{\infty} \frac{d\epsilon'}{2\pi} e^{-i(\epsilon - \epsilon')t} \text{Tr}_4 \left\{ \hat{\tau}_z \hat{d}^<(\epsilon, \epsilon') \right\}, \quad (3)$$

where  $\text{Tr}_4$  is trace over spin $\otimes$ particle-hole space,  $\hat{\tau}_z$  the Pauli matrix, and  $\hat{d}^< = [\hat{d}^K - (\hat{d}^R - \hat{d}^A)]/2$  with  $\hat{d}^{R,A,K}$  the retarded, advanced, Keldysh components of  $\check{d}$ , respectively. Since  $(\hat{d}^R - \hat{d}^A)$  is proportional to the density of states, it does not contribute to the total current. One can find the explicit form of  $\hat{d}^K$  after some algebra and then calculate the current  $I(t)$ . These calculations are outlined in the Appendix. Choosing the origin of time so that the superconducting phase  $\phi = 0$  at  $t = 0$ , we express the current as a sum over its Fourier components in harmonics of the Josephson frequency  $2eV$

$$I(t) = \sum_{n=-\infty}^{\infty} I_n e^{-2ineVt}, \quad (4)$$

where the current components are given by (taking  $k_B = 1$ )

$$I_n = \frac{V}{R_N} \delta_{n0} + \frac{1}{eR_N} \int_{-\infty}^{\infty} d\epsilon \tanh\left(\frac{\epsilon}{2T}\right) J_n(\epsilon) \quad (5)$$

with  $R_N^{-1} = e^2 D / \pi$  the normal conductance. Here  $J_n(\epsilon)$  is the  $n$ -th harmonics of the current density, which has a complicated structure given in the Appendix. In the tunneling limit ( $D \ll 1$ ), one can easily reproduce previous analytical results from these formulas.<sup>15</sup> Since the current  $I(t)$  is real, it follows that the current components satisfy  $I_n^* = I_{-n}$ . Therefore, alternatively one can express Eq. (4) as

$$I(t) = I_0 + \sum_{n=1}^{\infty} \{ I_n^c \cos(2neVt) + I_n^s \sin(2neVt) \}, \quad (6)$$

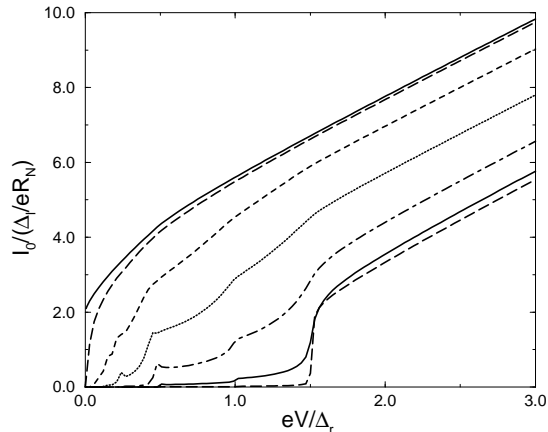


FIG. 2: The dc ( $n = 0$ ) current component for asymmetric junctions ( $\Delta_l/\Delta_r = 0.5$ ) at different transmission coefficients (lower to upper curves)  $D = 0.01, 0.1, 0.4, 0.7, 0.9, 0.99$ , and 1 at zero temperature. In all figures we set the parameter for inelastic scattering rate  $\eta = 10^{-5}\Delta_r$ .

where  $I_n^c \equiv 2\text{Re}\{I_n\}$  and  $I_n^s \equiv 2\text{Im}\{I_n\}$ . In the following, we shall call the  $n = 1$  components  $I_1^c$  and  $I_1^s$ , respectively, the cosine and the sine components.

Applying the formulas obtained above, one can calculate the current components  $I_n$  for general transmission coefficient  $D$  at arbitrary bias voltages  $V$  for any temperature  $T$ . In the following section, we shall demonstrate numerical results for the first two current components  $I_0$  and  $I_1$ . In particular, we shall study in detail the regime where the dynamics of the Andreev bound-states is important. This corresponds to the low bias limit for which quasiparticle damping is extremely weak. Namely, we will be interested in the regime where the inelastic scattering rate  $\eta$  (see Eq. (A 2) in the Appendix) is vanishingly small, so that  $\eta \ll eV \ll \Delta_l$ .<sup>11,12</sup>

### III. CURRENT COMPONENTS

We shall now study numerical results obtained from the formulas derived in the previous section. We will first examine the current components at zero temperature and then consider the temperature dependence of the dc component at the end of this section. In all numerical results presented below, unless stated otherwise, we choose the gap ratio  $\Delta_l/\Delta_r = 0.5$  and take the inelastic scattering rate  $\eta = 10^{-5}\Delta_r$  for the calculations.

Figure 2 shows the zero temperature results for the dc components  $I_0$  at different transmission coefficients  $D$  in the asymmetric junction. As was found previously,<sup>7</sup> for  $D = 1$  the dc component  $I_0$  has a finite interception  $2e\Delta_l/\pi$  at low bias. For bias below  $(\Delta_l + \Delta_r)$ , due to multiple Andreev reflections, there are subgap structures which are richer than the equal gap case owing to the

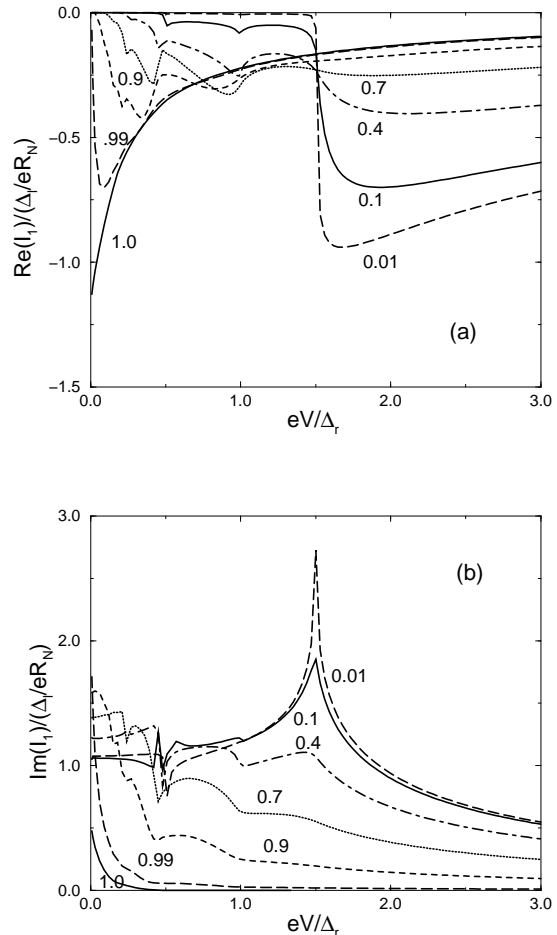


FIG. 3: The zero temperature results for (a) the real and (b) the imaginary parts of the current components  $I_1$  for asymmetric junctions ( $\Delta_l/\Delta_r = 0.5$ ) at different junction transparencies.

presence of two gaps. These structures can be classified as detailed in Ref. 7 and we shall not repeat it here.

Figure 3 shows the real and the imaginary parts of the current component  $I_1$  at zero temperature. The general features are very similar to the equal gap case (cf. Fig. 2 in Ref. 8). In the present case, however, the current components undergo larger oscillations in the subgap region than the equal gap results. Moreover, for  $D = 1$  the imaginary part of  $I_1$  (and hence the sine component  $I_1^s$ ) can take non-zero values – in contrast to the equal gap case, where the sine component vanishes identically.<sup>8</sup> We shall see below that in the low bias limit this finite sine component can be understood by generalizing the picture obtained by Averin and Bardas<sup>8</sup> to the unequal gap situation. Namely, we will show that the non-zero sine component originates from qualitative changes in the current-phase relation when the gap ratio is not one. It will be seen that the contribution arises completely from the continuum states.

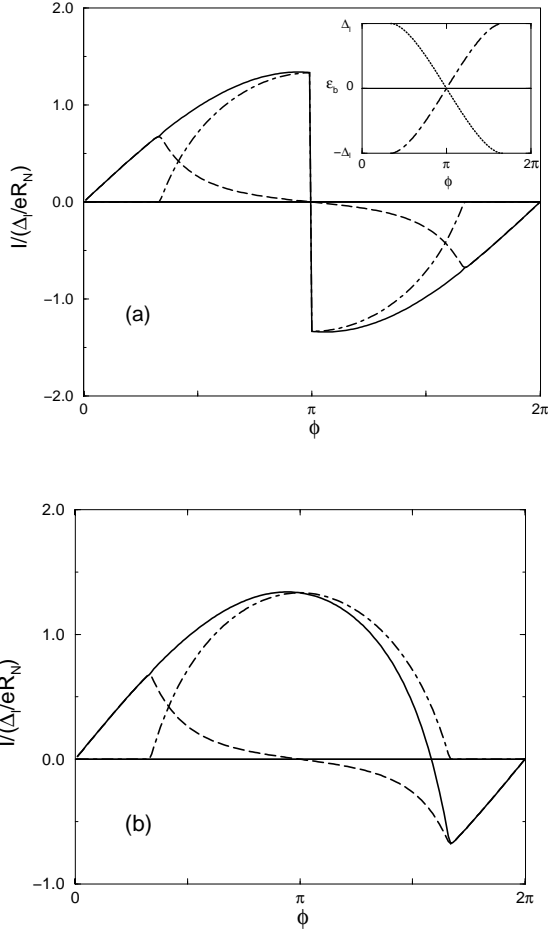


FIG. 4: The zero temperature current-phase relations for ballistic junctions ( $D = 1$ ) with gap ratio  $\Delta_l/\Delta_r = 0.5$  (a) in equilibrium ( $V = 0$ ) and (b) at low bias ( $V \rightarrow 0$ ). The total current (full lines) and the current contributions from the bound states (dot-dashed lines) and the continuum states (dashed lines) are shown. Note that the continuum contributions remain the same, whereas there is no branch switching for the bound state for  $V \neq 0$  (see text). The inset in (a) displays the bound-state spectra for the particle right-moving (dot-dashed line) and left-moving (dotted line) branches. Note that the bound states do not exist for some ranges of  $\phi$ .<sup>5,6</sup>

As pointed out by Averin and Bardas for equal gap junctions,<sup>8</sup> at low bias the ac current components can be related to the Fourier components of the current-phase relation. For equal gap junctions, the supercurrent is carried entirely by the Andreev bound-states. For unequal gap junctions, however, apart from the bound states, the continuum states ( $\Delta_l < |\epsilon| < \Delta_r$ ) can also contribute to the current.<sup>5,6</sup> As shown in Fig. 4(a)(b), the continuum contributions behave the same under zero and finite bias. In particular, the continuum contribution is always odd with respect to  $\phi = \pi$ . For the bound-state contributions, however, the situation is quite different, as we shall

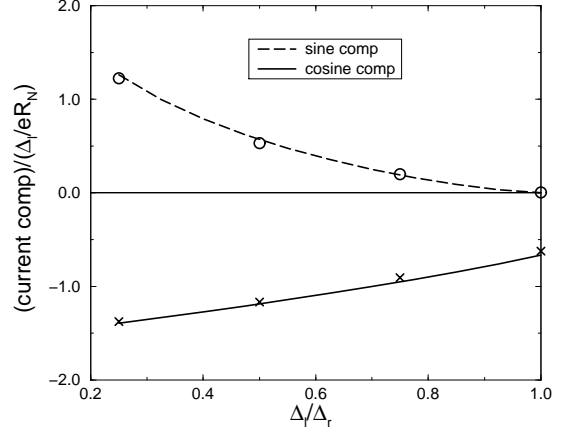


FIG. 5: The variation of the first Fourier components at low bias with respect to gap ratio for ballistic ( $D = 1$ ) junctions. The lines depict the first Fourier components of the current-phase relation, while the symbols are the real (crosses) and imaginary (circles) parts of the current component  $I_1$ . The deviations at small gap ratios are due to numerical difficulties in low-bias calculations for  $I_1$ . Note that for unequal gaps, the sine component is no longer zero.

now explain.

The two branches of the Andreev bound-states carry supercurrent in opposite directions and only one of them can be occupied (see inset of Fig. 4(a)). In equilibrium, since the chemical potential lies in the middle of the energy gap ( $\epsilon = 0$ ), it is always the lower branch that is occupied. Therefore in this case, as shown in Fig. 4(a), the bound-state contribution always switches branch when the superconducting phase  $\phi$  goes across  $\pi$ .<sup>5</sup> In the presence of finite bias, however, since the phase evolves according to the Josephson relation ( $d\phi/dt = 2eV$ ), the bound-state current always follows a single branch of the bound-state spectra, so that the corresponding current contribution remains the same sign during one period.<sup>8</sup> Figure 4(b) shows the low-bias effective current-phase relation for ballistic junctions with gap ratio  $\Delta_l/\Delta_r = 0.5$ . Since there is no branch switching, the bound-state current stays positive and is even with respect to  $\phi = \pi$ . On the other hand, due to the finite gap for the continuum states, their contributions is the same as the  $V = 0$  case and remains odd with respect to  $\phi = \pi$ . Since  $\sin\phi$  is an odd function with respect to  $\phi = \pi$ , the sine transform of the low bias current-phase relation is thus non-zero due entirely to the continuum-state contributions.

To verify this picture, we show in Figure 5 a comparison between  $I_1$  and the first Fourier components of the low-bias effective current-phase relation of Fig. 4(b) for ballistic junctions at different gap ratios. One can observe that they match well with each other. The sine components become non-zero when the gap ratio is not equal to one. As pointed out above, this can be under-

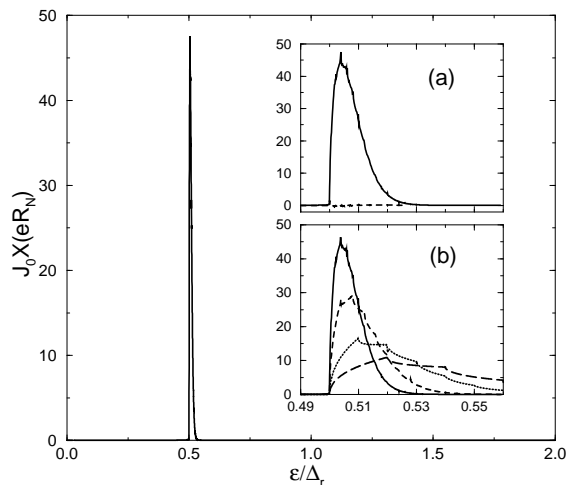


FIG. 6: The current densities  $J_0$  for asymmetric junctions with  $\Delta_l/\Delta_r = 0.5$ . We plot only the region  $\epsilon > 0$  since the current density can be taken an odd function of energy (the even part will not survive the integral in Eq. (5)). The main panel shows the plot for  $D = 1$  at bias  $eV = 10^{-3}\Delta_r$ . Inset (a) shows current density near the smaller gap for  $D = 1$  (solid line) and  $D = 0.99$  (dashed line). Inset (b) shows current densities for  $D = 1$  at different bias voltages  $eV/\Delta_r = 10^{-3}$  (solid line),  $2 \times 10^{-3}$  (dashed line),  $5 \times 10^{-3}$  (dotted line), and  $10 \times 10^{-3}$  (long dashed line).

stood from the current-phase relation and is entirely due to the continuum states. This result thus confirms that the picture obtained in Ref. 8 can be extended to unequal gap junctions. Also, it illustrates the importance of continuum-state contributions to the ac current components in unequal gap junctions.

Finally, we study the temperature dependence of the dc component for ballistic junctions in the low bias limit. In the equal gap case, it was shown by Averin and Bardas<sup>8</sup> that in the low bias limit, the current receives major contributions from the neighborhood ( $\sim eV$ ) of the gap edges. This is because particles and holes with incident energies in these ranges can undergo divergent numbers of Andreev reflections (of order  $\Delta/eV$ ) which generate dominant contributions to the current. Therefore, it follows that the temperature dependence of the current is determined by the occupation factor near the gap edge. We shall now generalize this picture to the unequal gap configurations.

To achieve this, we plot in Fig. 6 the current density  $J_0$  for the dc component at small bias for  $D = 1$ . It is clearly seen that the current density has a sharp peak near the smaller gap  $\Delta_l$ . Therefore, from Eq. (5), one concludes easily that the temperature dependence of the dc component is determined from the quasiparticle occupation near the *smaller gap*. This is confirmed by the plot shown in Fig. 7, where it is seen that the result fits well with the expression  $(2e\Delta_l/\pi) \tanh(\Delta_l/2T)$ . Indeed the reason for the sharp peak near the smaller gap is very similar to its equal gap counterpart. Namely, at low

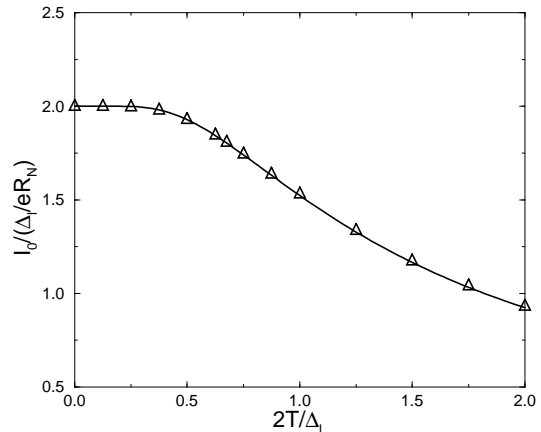


FIG. 7: Temperature dependence of the dc component  $I_0$  at low bias for a ballistic asymmetric junction ( $\Delta_l/\Delta_r = 0.5$ ). The triangles are results obtained from our expression and the solid line is the curve  $(2e\Delta_l/\pi) \tanh(\Delta_l/2T)$ . Here the bias voltage set at  $eV = 10^{-3}\Delta_r$ .

bias, excitations near the smaller gap are being injected into the point contact and “become” the Andreev bound state: they undergo a divergent number of Andreev reflections for  $V \rightarrow 0$ . For particles and holes with incident energies between the smaller and larger gaps, they are only partially Andreev reflected and hence contribute insignificantly to the current as  $V \rightarrow 0$ . The presence of finite reflection can reduce the current density near the smaller gap significantly; this is illustrated in inset (a) of Fig. 6. Also, when the bias increases, the peak at the smaller gap broadens (see inset (b) of Fig. 6) and the current receives contributions from a wider range of energies. Eventually, when the bias is large the picture described above becomes no longer valid.

In closing this section, we would like to point out an interesting feature which appears in the plots for the current densities. As can be seen clearly from insets (a) and (b) of Fig. 6, there are regular steps (or shoulders) in the current density profiles which are separated by  $2eV$ . Indeed these steps are consequences of the change in the number of Andreev reflections when varying the energy of the incident particles. Their occurrence thus further supports the picture presented above.

#### IV. SUMMARY AND DISCUSSION

We have studied the ac Josephson effect in asymmetric superconducting quantum point contacts, where the gap amplitudes on the two superconducting electrodes are different. Applying the quasiclassical method, we are able to derive formulas applicable to general transmission coefficient  $D$  and arbitrary bias voltages. We calculate the  $IV$  curves for general  $D$  and study in detail the low

bias limit, where quasiparticle damping can be ignored. We find in this limit for ballistic junctions ( $D = 1$ ) that the sine component becomes non-zero once the two superconducting gaps become unequal. By comparing the results with the Fourier components of the current-phase relation, we are able to confirm that the non-zero sine component is entirely due to the continuum states. In the same limit, we also find that the temperature dependence of the dc component is determined by the occupation factor at the smaller gap. These results confirm that the picture obtained by Averin and Bardas<sup>8</sup> can be generalized to the case of asymmetric junctions.

Finally, to test our results for the non-vanishing sine component for unequal gap junctions, it is necessary to measure the current component  $I_1$  experimentally. As suggested by Hurd *et al.*,<sup>7</sup> this may be achieved by using a proper phase-biasing network. Moreover, in the presence of a microwave radiation, it may also have consequences on the subharmonic Shapiro steps.<sup>16</sup> An interesting issue which is not addressed in this article is the change in the non-equilibrium noise (shot noise) when the Andreev bound-states are missing in asymmetric junctions. This will be the subject of our future publication.

### Acknowledgments

We would like to thank Professor A. D. Zaikin for comments. This research was supported by NSC of Taiwan under grant numbers NSC 91-2112-M-001-063 and 92-2811-M-001-040.

## APPENDIX

In this appendix we outline the essential elements for the calculation of the current components  $I_n$ . We supply the explicit expressions for the Green's functions and explain the schemes for the numerical calculation of the matrix element  $\hat{d}^K$ . Finally, we display the explicit formula for the current density  $J_n$ .

### 1. The Green's functions

Since we do not consider magnetic phenomena in the present work, the spin degrees of freedom merely introduce a factor of two (cf. Ref. 17). The Green's functions we shall be dealing with are hence reduced to the Keldysh  $\otimes$  particle-hole space. Since the superconducting electrode on the left remains in equilibrium, the retarded ( $R$ ) and the advanced ( $A$ ) Green's functions in frequency space are ( $\alpha = R, A$ )

$$\hat{g}_{l\infty}^\alpha(\epsilon, \epsilon') = 2\pi\delta(\epsilon - \epsilon') [\hat{\tau}_z g_l^\alpha(\epsilon) - i\hat{\tau}_y f_l^\alpha(\epsilon)] . \quad (\text{A } 1)$$

Here  $\hat{\tau}_i$  are Pauli matrices in the particle-hole space; the functions  $g_l$  and  $f_l$  are

$$\begin{aligned} g_l^{R,A}(\epsilon) &= -\pi \frac{\epsilon \pm i\eta}{\sqrt{\Delta_l^2 - (\epsilon \pm i\eta)^2}} \\ f_l^{R,A}(\epsilon) &= -\pi \frac{\Delta_l}{\sqrt{\Delta_l^2 - (\epsilon \pm i\eta)^2}} \end{aligned} \quad (\text{A } 2)$$

with  $\eta$  a small positive number related to the inelastic scattering rate. The Keldysh Green's function is given by

$$\hat{g}_l^K = \hat{g}_l^R \hat{n}_l - \hat{n}_l \hat{g}_l^A \quad (\text{A } 3)$$

with  $\hat{n}_l$  the distribution function

$$\hat{n}_l(\epsilon, \epsilon') = 2\pi\delta(\epsilon - \epsilon') n(\epsilon) \hat{1}, \quad (\text{A } 4)$$

where  $n(\epsilon) = \tanh(\epsilon/2T)$ .

In the presence of bias voltage  $V$ , the superconducting phase becomes time dependent. The non-equilibrium Green's function  $\check{g}$  can be obtained from the equilibrium Green's function  $\check{g}_\infty$  through the following transformation

$$\begin{aligned} \check{g}(t, t') &= \check{S}(t) \check{g}_\infty(t - t') \check{S}^\dagger(t'), \\ &= \begin{pmatrix} \hat{S}(t) & 0 \\ 0 & \hat{S}(t) \end{pmatrix} \begin{pmatrix} \hat{g}_\infty^R & \hat{g}_\infty^K \\ 0 & \hat{g}_\infty^A \end{pmatrix} \begin{pmatrix} \hat{S}^\dagger(t') & 0 \\ 0 & \hat{S}^\dagger(t') \end{pmatrix}, \end{aligned} \quad (\text{A } 5)$$

where

$$\hat{S}(t) = \begin{pmatrix} e^{i\Phi(t)} & 0 \\ 0 & e^{-i\Phi(t)} \end{pmatrix} \quad (\text{A } 6)$$

with the time dependent phase  $\Phi(t) = \phi_0/2 + eVt$ .

Therefore, for the superconducting electrode on the right, expressing  $\hat{\tau}_\pm = (\hat{\tau}_x \pm i\hat{\tau}_y)/2$ , one can find for  $\alpha = R, A$

$$\begin{aligned} \hat{g}_r^\alpha(\epsilon, \epsilon') &= 2\pi \left[ \hat{\tau}_z \delta(\epsilon - \epsilon') g_r^\alpha(\epsilon + \tau_z eV) \right. \\ &\quad \left. - \hat{\tau}_+ \delta(\epsilon - \epsilon' + 2eV) f_r^\alpha(\epsilon + eV) e^{i\phi_0} \right. \\ &\quad \left. + \hat{\tau}_- \delta(\epsilon - \epsilon' - 2eV) f_r^\alpha(\epsilon - eV) e^{-i\phi_0} \right] \quad (\text{A } 7) \end{aligned}$$

In this expression,  $g_r^{R,A}$  and  $f_r^{R,A}$  are the same as (A 2) after replacing the subscript  $l$  by  $r$  there. Similarly, the Keldysh Green's function  $\hat{g}_r^K$  can be obtained in the same way as (A 3) with the replacement of all subscripts  $l$  by  $r$  and using the distribution function

$$\hat{n}_r(\epsilon, \epsilon') = 2\pi\delta(\epsilon - \epsilon') \begin{pmatrix} n(\epsilon + eV) & 0 \\ 0 & n(\epsilon - eV) \end{pmatrix}, \quad (\text{A } 8)$$

where  $n(\epsilon)$  is the same as in (A 4).

## 2. The matrix $\hat{d}^K$

To calculate the current, we shall need the Keldysh component of the quantity  $\hat{d}$  which can be found from Eq. (2)

$$\begin{aligned} \hat{d}^K = & \frac{iD}{2\pi} \left\{ \hat{g}_r^R \hat{g}_{l,\infty}^K + \hat{g}_r^K \hat{g}_{l,\infty}^A - \hat{g}_{l,\infty}^R \hat{g}_r^K - \hat{g}_{l,\infty}^K \hat{g}_r^A \right. \\ & \left. - \frac{D}{4\pi^2} [\hat{g}_r^R, \hat{g}_{l,\infty}^R] \hat{Q}^R (\hat{g}_r^R \hat{g}_r^K + \hat{g}_r^K \hat{g}_r^A) \right\} \\ & \times \hat{Q}^A, \end{aligned} \quad (\text{A } 9)$$

where  $\hat{g}_-^\alpha \equiv (\hat{g}_r^\alpha - \hat{g}_{l,\infty}^\alpha)$  and  $\hat{Q}^\alpha \equiv \left[ \hat{1} + \frac{D}{4\pi^2} (\hat{g}_-^\alpha)^2 \right]^{-1}$  for  $\alpha = R, A$ . As usual, convolution over the energy variables is understood in the above formula. To obtain the explicit form for  $\hat{d}^K$ , it is necessary to calculate the quantity  $\hat{Q}$ . To proceed, we note first that, using the normalization condition  $(\hat{g})^2 = -\pi^2 \hat{1}$ , one can find

$$\begin{aligned} \hat{Q} &= \left( \frac{2}{2-D} \right) \left[ \hat{1} - \frac{D}{2\pi^2(2-D)} \{ \hat{g}_{l,\infty}, \hat{g}_r \} \right]^{-1} \\ &\equiv \left( \frac{2}{2-D} \right) \hat{H}^{-1}. \end{aligned} \quad (\text{A } 10)$$

As usual,  $\{\hat{a}, \hat{b}\} = \hat{a}\hat{b} + \hat{b}\hat{a}$  is the anticommutator. Note that for brevity here and below we omit the superscripts  $R, A$  for the retarded and advanced functions.

Using the explicit expressions for  $\hat{g}_{l,\infty}^\alpha$  and  $\hat{g}_r^\alpha$  given above, one can express  $\hat{H}$  in frequency space as

$$\begin{aligned} \hat{H}(\epsilon, \epsilon') = & 2\pi \left[ \delta(\epsilon - \epsilon') \hat{H}^0 + \delta(\epsilon - \epsilon' - 2eV) \hat{H}^+ \right. \\ & \left. + \delta(\epsilon - \epsilon' + 2eV) \hat{H}^- \right]. \end{aligned} \quad (\text{A } 11)$$

We note that in frequency space  $\hat{H}$  possesses the structure of a “tight-binding Hamiltonian”.<sup>12,18</sup> Therefore, we use the ansatz for its inverse  $\hat{Q}$

$$\hat{Q}(\epsilon, \epsilon') = \sum_{m=-\infty}^{\infty} 2\pi \delta(\epsilon - \epsilon' - 2meV) \hat{Q}_m(\epsilon'). \quad (\text{A } 12)$$

The equation  $\hat{H}\hat{Q} = \hat{1}$  immediately leads to

$$\hat{H}_m^0 \hat{Q}_m + \hat{H}_m^+ \hat{Q}_{m-1} + \hat{H}_m^- \hat{Q}_{m+1} = \delta_{m0} \hat{1}, \quad (\text{A } 13)$$

where we have denoted  $\hat{H}^\pm(\epsilon, \epsilon \mp 2eV) \equiv \hat{H}_m^\pm$  and  $\hat{H}^0(\epsilon, \epsilon) \equiv \hat{H}_m^0$ ; note that here  $\epsilon = \epsilon' + 2meV$  and that we have taken  $\epsilon'$  as the “origin”  $m = 0$ .

To solve (A 13), we define the transfer matrices  $\hat{t}_m^\pm$  so that

$$\begin{aligned} \hat{t}_m^+ \hat{Q}_m &= \hat{Q}_{m+1}, & m \geq 0; \\ \hat{t}_m^- \hat{Q}_m &= \hat{Q}_{m-1}, & m \leq 0. \end{aligned} \quad (\text{A } 14)$$

For  $m \neq 0$  Eq. (A 13) becomes a homogeneous equation, from which one can derive the following recursion relations for the transfer matrices

$$\begin{aligned} \hat{t}_m^+ &= - \left( \hat{H}_{m+1}^0 + \hat{H}_{m+1}^- \hat{t}_{m+1}^+ \right)^{-1} \hat{H}_{m+1}^+, & m \geq 0; \\ \hat{t}_m^- &= - \left( \hat{H}_{m-1}^0 + \hat{H}_{m-1}^+ \hat{t}_{m-1}^- \right)^{-1} \hat{H}_{m-1}^-, & m \leq 0. \end{aligned} \quad (\text{A } 15)$$

We solve the transfer matrices  $\hat{t}_m^\pm$  numerically by truncating the recursion relations (A 15) at  $|m| \sim \Delta_r/(eV)$ . This means that we are ignoring Andreev reflections when the energy is cycled above the gap edges (we choose the larger gap  $\Delta_r$  to improve convergence in the numerical results). This is justified since the Andreev reflection coefficients decay very quickly above the energy gap. One can thus obtain the solution at  $m = 0$

$$\hat{Q}_0 = \left( \hat{H}_0^0 + \hat{H}_0^+ \hat{t}_0^- + \hat{H}_0^- \hat{t}_0^+ \right)^{-1}. \quad (\text{A } 16)$$

Applying (A 14), we can construct  $\hat{Q}_m$  for all values of  $m$  and hence obtain  $\hat{Q}^{R,A}$  using (A 12). Substituting the results back into (A 10) and (A 9), we can then find the expression for  $\hat{d}^K$ . One can thus obtain Eqs. (4) and (5) by making use of (3). The explicit form for the  $n$ -th harmonic  $J_n$  of the current density is given in the following section.

## 3. current density

For completeness, we provide the explicit expression for the current density in this section. We first denote the  $R, A, K$  components of the commutator

---


$$[\hat{g}_r, \hat{g}_{l,\infty}]^\alpha(\epsilon, \epsilon') = 2\pi \left( \delta(\epsilon - \epsilon') \hat{M}_0^\alpha(\epsilon) + \delta(\epsilon - \epsilon' - 2eV) \hat{M}_+^\alpha(\epsilon) + \delta(\epsilon - \epsilon' + 2eV) \hat{M}_-^\alpha(\epsilon) \right) \quad (\text{A } 17)$$

and similarly

$$\left(\hat{g}_-^R \hat{g}_-^K + \hat{g}_-^K \hat{g}_-^A\right)(\epsilon, \epsilon') = 2\pi \left(\delta(\epsilon - \epsilon') \hat{N}_0^K(\epsilon) + \delta(\epsilon - \epsilon' - 2eV) \hat{N}_+^K(\epsilon) + \delta(\epsilon - \epsilon' + 2eV) \hat{N}_-^K(\epsilon)\right). \quad (\text{A } 18)$$

The explicit forms of the matrix elements  $\hat{M}_{0,\pm}^\alpha$ ,  $\hat{N}_{0,\pm}^K$  can be obtained by applying the expressions for  $\hat{g}_r^\alpha$  and  $\hat{g}_{l,\infty}^\alpha$  given in Sec. 1 of this Appendix. It is convenient to decompose the Keldysh components  $\hat{M}_{0,\pm}^K$  according to their dependence on the distribution function  $n(\epsilon)$  as

$$\hat{M}_0^K(\epsilon) = \hat{M}_0^{K0}(\epsilon) n(\epsilon) + \hat{M}_0^{K+1}(\epsilon) n(\epsilon + eV) + \hat{M}_0^{K-1}(\epsilon) n(\epsilon - eV), \quad (\text{A } 19)$$

$$\hat{M}_+^K(\epsilon) = \hat{M}_+^{K0}(\epsilon) n(\epsilon) + \hat{M}_+^{K-1}(\epsilon) n(\epsilon - eV) + \hat{M}_+^{K-2}(\epsilon) n(\epsilon - 2eV), \quad (\text{A } 20)$$

$$\hat{M}_-^K(\epsilon) = \hat{M}_-^{K0}(\epsilon) n(\epsilon) + \hat{M}_-^{K+1}(\epsilon) n(\epsilon + eV) + \hat{M}_-^{K+2}(\epsilon) n(\epsilon + 2eV), \quad (\text{A } 21)$$

and similarly for  $\hat{N}_{0,\pm}^K$ . Using (A 10), (A 12), together with (A 17)–(A 21) in (A 9) and (3), and then shifting the dummy variables so that all occupation factors become  $n(\epsilon)$ , one can obtain (5) and find

$$J_n(\epsilon) = \frac{1}{16\pi^2(2-D)} \times \left\{ \text{Tr}_4 \left[ \hat{\tau}_z \hat{\mathcal{A}}(\epsilon) \right] - \frac{D}{2\pi^2(2-D)} \sum_{m=-\infty}^{\infty} \text{Tr}_4 \left[ \hat{\tau}_z \hat{\mathcal{B}}_m(\epsilon) \right] \right\}, \quad (\text{A } 22)$$

where

$$\begin{aligned} \hat{\mathcal{A}}(\epsilon) &= \hat{M}_0^{K0}(\epsilon) \hat{\mathcal{Q}}_n^A(\epsilon_n) + \hat{M}_+^{K0}(\epsilon) \hat{\mathcal{Q}}_{n-1}^A(\epsilon_n) + \hat{M}_-^{K0}(\epsilon) \hat{\mathcal{Q}}_{n+1}^A(\epsilon_n) \\ &+ \hat{M}_0^{K+1}(\epsilon - eV) \hat{\mathcal{Q}}_n^A(\epsilon_n - eV) + \hat{M}_-^{K+1}(\epsilon - eV) \hat{\mathcal{Q}}_{n+1}^A(\epsilon_n - eV) + \hat{M}_-^{K+2}(\epsilon - 2eV) \hat{\mathcal{Q}}_{n+1}^A(\epsilon_n - 2eV) \\ &+ \hat{M}_0^{K-1}(\epsilon + eV) \hat{\mathcal{Q}}_n^A(\epsilon_n + eV) + \hat{M}_+^{K-1}(\epsilon + eV) \hat{\mathcal{Q}}_{n-1}^A(\epsilon_n + eV) + \hat{M}_+^{K-2}(\epsilon + 2eV) \hat{\mathcal{Q}}_{n-1}^A(\epsilon_n + 2eV) \end{aligned} \quad (\text{A } 23)$$

and

$$\begin{aligned} \hat{\mathcal{B}}_m(\epsilon) &= \hat{\mathcal{M}}(\epsilon + 2meV) \left[ \hat{N}_0^{K0}(\epsilon) \hat{\mathcal{Q}}_{n-m}^A(\epsilon_{n-m}) + \hat{N}_+^{K0}(\epsilon) \hat{\mathcal{Q}}_{n-m-1}^A(\epsilon_{n-m}) + \hat{N}_-^{K0}(\epsilon) \hat{\mathcal{Q}}_{n-m+1}^A(\epsilon_{n-m}) \right] \\ &+ \hat{\mathcal{M}}(\epsilon + (2m-1)eV) \left[ \hat{N}_0^{K+1}(\epsilon - eV) \hat{\mathcal{Q}}_{n-m}^A(\epsilon_{n-m} - eV) + \hat{N}_-^{K+1}(\epsilon - eV) \hat{\mathcal{Q}}_{n-m+1}^A(\epsilon_{n-m} - eV) \right] \\ &+ \hat{\mathcal{M}}(\epsilon + (2m+1)eV) \left[ \hat{N}_0^{K-1}(\epsilon + eV) \hat{\mathcal{Q}}_{n-m}^A(\epsilon_{n-m} + eV) + \hat{N}_+^{K-1}(\epsilon + eV) \hat{\mathcal{Q}}_{n-m-1}^A(\epsilon_{n-m} + eV) \right] \\ &+ \hat{\mathcal{M}}(\epsilon + 2(m+1)eV) \hat{N}_+^{K-2}(\epsilon + 2eV) \hat{\mathcal{Q}}_{n-m-1}^A(\epsilon_{n-m-1}) \\ &+ \hat{\mathcal{M}}(\epsilon + 2(m-1)eV) \hat{N}_-^{K+2}(\epsilon - 2eV) \hat{\mathcal{Q}}_{n-m+1}^A(\epsilon_{n-m+1}). \end{aligned} \quad (\text{A } 24)$$

In the above expressions, we have denoted  $\epsilon_n \equiv \epsilon - 2neV$  and

$$\hat{\mathcal{M}}(\epsilon) \equiv \hat{M}_0^R(\epsilon) \hat{\mathcal{Q}}_m^R(\epsilon_m) + \hat{M}_+^R(\epsilon) \hat{\mathcal{Q}}_{m-1}^R(\epsilon_m) + \hat{M}_-^R(\epsilon) \hat{\mathcal{Q}}_{m+1}^R(\epsilon_m). \quad (\text{A } 25)$$

<sup>1</sup> See, for example, M. Tinkham, Introduction to superconductivity, 2nd ed. (McGraw-Hill, New York, 1996).

<sup>2</sup> H. Takayanagi, T. Akazaki, and J. Nitta, Phys. Rev. Lett. **75**, 3533 (1995).

<sup>3</sup> N. van der Post, E. T. Peters, I. K. Yanson, and J. M. van Ruitenbeek, Phys. Rev. Lett. **73**, 2611 (1994); E. Scheer, P. Joyez, D. Esteve, C. Urbina, and M. H. Devoret, *ibid*

**78**, 3535 (1997); E. Scheer, N. Agrait, J. C. Cuevas, A. L. Yeyati, B. Ludoph, A. Martín-Rodero, G. R. Bollinger, J. M. van Ruitenbeek, and C. Urbina, Nature **394**, 154 (1998); B. Ludoph, N. van der Post, E. N. Bratus', E. V. Bezuglyi, V. S. Shumeiko, G. Wendin, and J. M. van Ruitenbeek, Phys. Rev. B **61**, 8561 (2000); M. F. Goffman, R. Cron, A. L. Yeyati, P. Joyez, M. H. Devoret, D. Esteve,



- and C. Urbina, Phys. Rev. Lett. **85**, 170 (2000).
- <sup>4</sup> A. Furusaki and M. Tsukada, Physica B **165** & **166**, 967 (1990); C. W. J. Beenakker, Phys. Rev. Lett **67**, 3836 (1991).
  - <sup>5</sup> L.-F. Chang and P. F. Bagwell, Phys. Rev. B **49**, 15853 (1994).
  - <sup>6</sup> S. K. Yip, Phys. Rev. B **68**, 024511 (2003).
  - <sup>7</sup> M. Hurd, S. Datta, and P. F. Bagwell, Phys. Rev. B **54**, 6557 (1996); *ibid.* **56**, 11232 (1997).
  - <sup>8</sup> D. Averin and A. Bardas, Phys. Rev. Lett **75**, 1831 (1995).
  - <sup>9</sup> For a general introduction to this method, see, for example, J. W. Serene and D. Rainer, Phys. Rep. **101**, 221 (1983), and J. Rammer and H. Smith, Rev. Mod. Phys. **58**, 323 (1986).
  - <sup>10</sup> A. V. Zaitsev and D. V. Averin, Phys. Rev. Lett. **80**, 3602 (1998).
  - <sup>11</sup> U. Günsenheimer and A. D. Zaikin, Phys. Rev. B **50**, 6317 (1994).
  - <sup>12</sup> J. C. Cuevas, A. Martín-Rodero, and A. L. Yeyati, Phys. Rev. B **54**, 7366 (1996).
  - <sup>13</sup> A. V. Zaitsev, Zh. Eksp. Theor. Fiz. **86**, 1742 (1984) [translation: Sov. Phys. JETP **59**, 1015 (1984)].
  - <sup>14</sup> S. K. Yip, J. Low. Temp. Phys. **109**, 547 (1997).
  - <sup>15</sup> N. R. Werthamer Phys. Rev. **147**, 255 (1966); A. I. Larkin and Yu. N. Ovchinnikov, Zh. Eksp. Theor. Fiz. **51**, 1535 (1966) [translation: Sov. Phys. JETP **24**, 1035 (1967)]. Note that in the latter reference, a sign error has occurred in their expression for  $I_1$  in Eq. (22), thus affecting their results in Eq. (23).
  - <sup>16</sup> J. C. Cuevas, J. Heurich, A. Martín-Rodero, A. L. Yeyati, and G. Schön, Phys. Rev. Lett. **88**, 157001 (2002).
  - <sup>17</sup> A. J. Millis, D. Rainer, and J. A. Sauls, Phys. Rev. B **38**, 4504 (1988).
  - <sup>18</sup> G. B. Arnold, J. Low. Temp. Phys. **68**, 1 (1987).